Method for distortion correction of multi-layered surface reconstruction using time-gated wavefront sensing approach

C. S. Tan
cstan@mmu.edu.my
Faculty of Engineering, Multimedia University, Cyberjaya 63100 Selangor, Malaysia

X. Wang
School of Engineering, Monash University Sunway Campus, 46150 Selangor, Malaysia

Y. H. Ng
Faculty of Engineering and Science, University of Tunku Abdul Rahman, 53300 Kuala Lumpur, Malaysia

W. K. Lim
Faculty of Engineering, Multimedia University, Cyberjaya 63100 Selangor, Malaysia

T. Y. Chai
Cardiovascular Imaging and Dynamics, UZ Herestraat 49 - box 7003, 3000 Leuven, Belgium

In order to estimate the multi-layer surface profile and to detect the inter-layer surfaces defects, gated wavefront sensing approach has been proposed in the previous works [1, 2]. However, the proposed methodology measures the wavefront that has been distorted by its prior surfaces (reflected wavefront) or post surfaces (transmitted wavefront). Analysis has to be performed to estimate the multi-layer wavefront sensing by taking into consideration the multi-layer surfaces condition. For reflected wavefront, the bottom layer(s) wavefront is (are) being distorted twice via separate interface points while traveling back to the lenslet arrays through our observation for the slope and phase measurement. The subsequent reconstructed surfaces are not accurate and corrected. Thus, a discrete layer correction technique for the surface reconstruction has been proposed to enhance the reconstruction accuracy by using the upper/top layer's wavefront information. This paper discusses on the case of 2-layer system, where the reflected wavefront from the bottom layer has been distorted and its surface reconstruction has been corrected. The results show that the distortion is significant and the correction is deemed necessary for industrial application such as in wafer warpage inter-layer profile estimation.
[DOI: http://dx.doi.org/10.2971/jeos.2013.13034]

Keywords: Gated Imaging, adaptive optics, microlens, multi-layered wavefront

1 INTRODUCTION

Semiconductor manufacturing processes require excellent surface flatness even during the early stage of the process. With the increasing gate density of 3D IC, Very Large Scale Integration (VLSI) designs and Ultra Large Scale Integration (ULSI) design, defects on a wafer surface or sub-surfaces are more likely to cause failures of chip production and lower yields, which is a significant problem considering the substantial financial investment in fabrication plants.Nevertheless, it is essential for semiconductor manufacturing to measure and control the topography of wafer surfaces at nanometer scale. In-plane geometrical defects on wafer surfaces extending laterally in the millimeter range and in vertically in the nanometer ranges are of increasing importance (enhancement of aspect ratio). It has been a severe yield limiting factor in future generation technologies due to this particular challenge. Thus, the wavefront sensing can be used for wafer inspection [1]–[4]. Raymond et al. [5] used a high performance Shack-Hartman sensor to analyze the wavefront of a beam of light reflected from a silicon wafer surface. By translating the wafer to analyze small portions of the wafer in each camera frame and then continuously piecing the frames together, sub-millimeter spatial resolution can be retained while rapidly analyzing large apertures. Nutschet et al. [6, 7] applied wavefront sensing technique to determine the flatness on bare and patterned wafer surfaces.

Other than the wavefront sensing approach, there are a few methods of non-destructive wafer surface inspections such as: dark-field inspection [8], reflectometry [9]–[13], ellipsometry [14]–[17], interferometry [2],[18]–[20] and second-harmonic generation [21]–[23]. In terms of the topographic analysis, not much has been done to find the interface of the second or the sub-layer of the material. Most of the tests focused on measuring the surface flatness for the first interface on the outermost surface of the material. The difficulties of deriving the second layer and its bottom interface are due to the lack of information given by the reflectance/transmittance of the light wave after it has propagated between the interfaces.

Lately, multi-layers wafer and integration is technically possible with the latest 3D IC technology. However, the researches using wavefront sensing techniques above do not address the inter-layer or multi-layer surface profile estimation or defect detection. Recently, Tuohy et al. [1] and Wang et al. [2] proposed depth-resolved and time-resolved wavefront aberrations estimation using a coherence-gated Shack-Hartmann

Received December 8, 2012; revised ms. received April 4, 2013; published May 26, 2013

ISSN 1990-2573

wave-front sensor respectively for general inspection purpose. However, they assumed that the multi-layer wavefront has not been distorted much by its inter-layer optical path. Specifically, the root cause analysis of wafer defect morphology will require actual 3D profile of the sub-layer defect from the early stage to the final product of the processes. Therefore, we propose a correction of surface reconstruction that propagates in the discrete layered medium. In order to describe the theory in its preliminary form, this paper reports the single dimension-2 layer system for a typical gated wavefront sensing setup. The objective of this research is to introduce the reconstructed surface correction that is needed in the gated wavefront sensing applications and its subsequent reconstruction works.

The rest of the paper is structured as follows: Section 2 highlights the general setup of a Gated Shack-Hartmann (GSH) wavefront sensing in time domain. Section 3 introduces the analytical model of the time gated wavefront sensing in a discrete interface medium. This is followed by a novel algorithm to compensate the multi-layer discrete medium effect for the wavefront that travels through the upper surfaces. Section 4 presents the results of the model by using 2-layer medium as the example. Section 5 concludes the results and findings.

2 THE GATED SHACK-HARTMANN (GSH) WAVEFRONT SENSING IN MULTI-LAYERED DESCRETE MEDIUM

The initial usage of the Shack-Hartmann Wavefront Sensor (SHWS) is in astronomical imaging. The application of this sensor in metrology, ophthalmic imaging and other research areas has been widely explored [1, 24, 25] since it is made available in the market due to the advancement of technology. Specifically, it is used to measure aberrations on the corneal surface [26] and the lens of the eye. From [4, 6], a typical wavefront sensing was illustrated that the reflection of a given surface is sampled in an array form. A deviation of the points from the centre of its respective grids indicates that the reflection has taken place on an uneven surface. Centroiding is used to measure such deviations. The array of points is known as the gradient of the wavefront of the surface received by the sensing device. The experiment by Raymond et al. [5] showed that the performance of the SHWS is very close to that of the interferometer.

The camera shuttering is also important in current research, as it captures the position of the light pulse when it propagates between the interfaces. Another advantage of these sensors is that they are less complex and less expensive compared to the interferometry. The calculation of reflection/transmission characteristics of a stratified material is explained and highlighted by various researchers [16],[27]–[33]. However, there are certain limitations on the calculations as the scattering and absorption that has not been taken into account during the process.

Various simulations have been done to predict the behavior of the light rays in a stratified material. A variation of reflectance changes over time in different multi-layered materials was simulated in the earlier paper, but with acoustic strain pulses [34]. Fujiwara et al. [16] demonstrated a total of four different silicon layers that are estimated in the ellipsometric test and the thickness obtained is compared to the TEM results, with marginal errors. Various layer estimations have been tested and the relative thickness of the layers was evaluated using the novel ellipsometric approach. This will allow them to retrieve the defect features/markers from its subsequent layers indirectly. Therefore, it is obvious that the multi-layer profile and surface evaluation is in higher demand recently, both in the industry application as well as in the fundamental research. However, none of them considered the distortions that will result in the absolute errors in the multi-layer surface reconstructions.

In order to time the gated multi-layers and apply the correction as proposed, we propose a system that consists of four major components, namely: pulsed laser, gated camera, optical assembly to align and guide the wavefront propagation and the Shack-Hartman lens arrays with its scanning stages. This paper proposes the correction needed at current gated wavefront system. However, the theory and setting of this research can be extended into various femto-second wavefront detection problems due to its nature of application in wafer inspection. This is a separate issue as it may involve non-linearity of material effects that is not the focus in this paper.

At current stage, we will focus on the correction technique that is essential for the subsequent research using the gated system as described below. For simplicity, as shown in Figure 1, only the Shack-Hartmann lenslet array, gated camera and collimating lenses are involved in the measurement. The system is based on the design from recent researches [5, 24] but it is coupled with a gated camera/sensor [35] to measure the time necessary for the light to propagate within the interfaces. It is assumed to be (but not limited) non-interferometric wavefront sensing approach, that only discrete reflection or diffraction was observed at the interface.

The calibration targets are machined to the desired accuracy. It consists of the light source and the collimator, a prism, well defined focusing lens, the testing specimen and the wavefront sensing assembly (e.g. Shack-Hartmann). Before the measurement, the calibration of the system should be carried out in multiple stages. Typical wavefront measurement steps are carried out for the gated system, except the reflectance is timed against its time of flight as well as its intensities profile. In femto-second laser, the non-linearity of the material might be a key consideration in future work. Thus, we limit the paper to introduce the correction technique due to the wavefront distortion in the priori discrete medium. The femto-second issues and optimization of wavefront estimation to achieve maximum accuracy will be addressed in future works.

The intensities of each reflectance (time gated of the layer reflectance) are then compared to its background images (captured before the testing sample is in place). The gate timing can be delayed and adjusted continuously to capture the frame/beam array returned from the surface of the material for each time interval. The gated timing of the camera represents the time of flight (in this paper, a single scattering reflec-

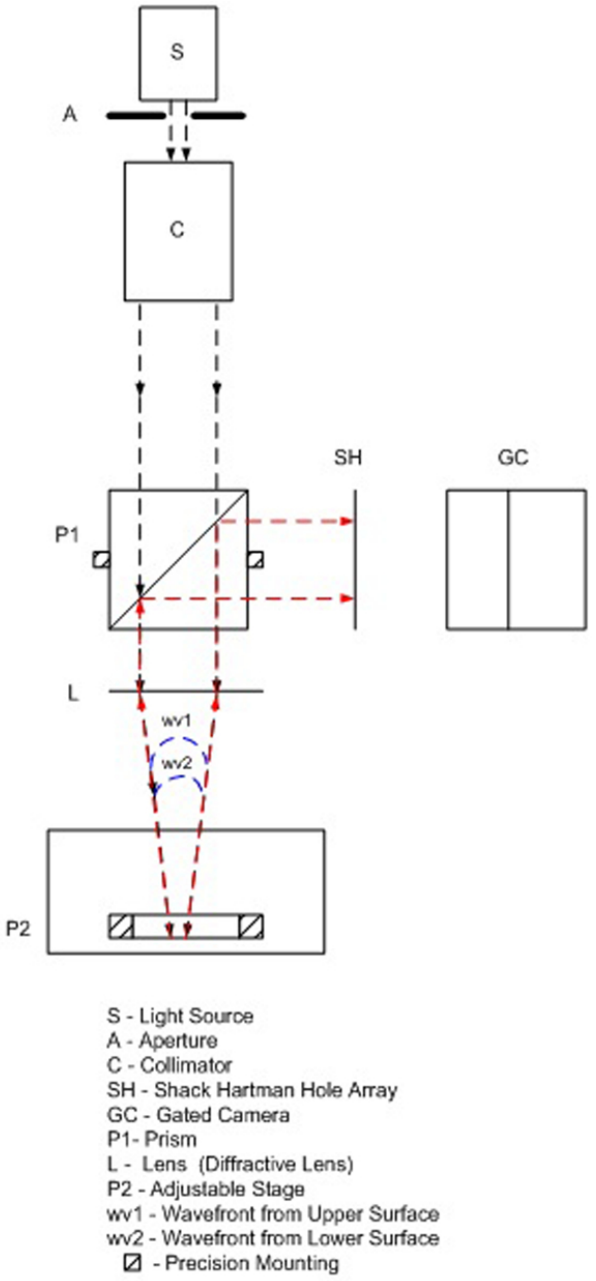

FIG. 1 Gated wavefront sensing system setup for 2 layers case.

tion is considered) of the particular layer wavefront reflection (for reflection case). On each interface, the respective coordinates and gradients are then fitted to a 3D surface by using Least Squares Method and Southwell's approximation [36].

The advantage of the proposed gated wavefront sensing is the simplicity of configuration and real-time processing ability for multi-layer discrete medium explicitly. Traditionally, the Shack-Hartmann wave-front sensor uses an array of micro-lens to dissect the incoming wave-front into segments [4] to create focal spots on a CCD array [37]. From the detection of these spots and consecutive integration of the displacements across the focal plane, the shape of the wavefront can be estimated.

The wave-front measurement is split into two parts, namely: range estimation, and wave-front reconstruction. The collimator and light source can be designed in any configuration provided that the wavefront is flat and orthogonal to the axis of traveling. The light will then pass through a series of components that are separated by a distance of half a pulse length for every optical element along the light path, r:

$$r = \frac{vt_0}{2}. \tag{1}$$

Where t_0 is the mean traveling time for a round trip to and from the surfaces, and v is the speed of light in the working condition. For simplicity, Busck's [38] approach is adopted to estimate the range of pixel data from the gated timing to achieve sub-micron accuracy.

The focusing lens L will focus the collimated beam on the testing surface. The reflected wave-front will travel in modulated/pulsed mode. Using Busck's approach, the mean target wavefront distance can be estimated from the wafer top and bottom surfaces, the wavefront reconstruction will be developed for the full top and bottom wafer surface by Southwell approach. This paper will not repeat Southwell and Busck methods, but highlight the compensation technique that can be used to identify the upper and bottom (2 layers system condition) wavefront.

The proposed system is a multi-layer wavefront sensing similar to the system proposed by Tuohy et al. [1], generally. However, compared to their system, the design is simpler and there will be fewer parts, thus cutting overall cost of the product. On top of that, only direct measurement is necessary in this system, whereas for the interferometry, some complex calculations including processing interferometric data are needed. In addition, the proposed system is less sensitive to vibrations [5] compared to their setup. Therefore, no extra algorithms to remove vibratory components are required in the phase output.

3 THE CORRECTION TECHNIQUE FOR GSH WAVEFRONT SENSING (2 LAYERS CASE)

The profile of the light field intensity on a multi-layered system can be estimated using Abeles' Matrix Method [39]. It should be noted that the discrete condition can be applied to stratified layered condition if each layer is treated with higher number of Abeles' transformation [40]. The wavefront propagation in multi-layer structure is investigated based on Fresnel formalism. The Fresnel formalism is obtained by applying Snell's law of refraction at all interfaces of wafer model (see Figure 2).

$$n_j \sin\theta_j = n_i \sin\theta_i. \tag{2}$$

Assume that there are N layers between medium 0 and medium $N+1$. Thus there is a total of $N+2$ media. In general, i.e., at n^{th} layer, there is an incoming and a reflected wave on the left side.

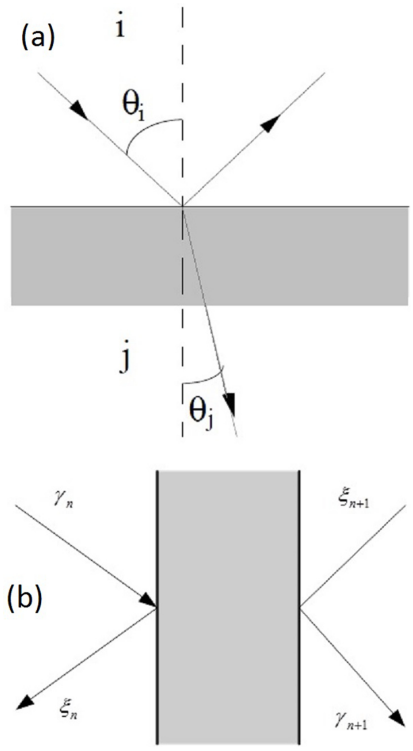

FIG. 2 (a) Illustration of Snell's law of refraction at an interface between materials (b) Reflections and transmissions in a given n layer.

γ_{n+1} and ξ_{n+1} are transmitted (for γ_0 , it will be incident wave) and reflected wave on layer $n+1$ (not shown in Figure 2, for multi layered case, they are projected to be exit/enter at the right hand side). Let us omit the phase part from Abeles's method. This relation can be expressed as:

$$\begin{pmatrix} \gamma_n \\ \xi_n \end{pmatrix} = \widetilde{M}_n \begin{pmatrix} \gamma_{n+1} \\ \xi_{n+1} \end{pmatrix}, \tag{3a}$$

$$\begin{pmatrix} \gamma_0 \\ \xi_0 \end{pmatrix} = \widetilde{M}_1 \cdot \widetilde{M}_2 \cdot \ldots \cdot \widetilde{M}_n \cdot \ldots \cdot \widetilde{M}_N \cdot \frac{1}{t_{N,N+1}} \begin{pmatrix} 1 & r_{N,N+1} \\ r_{N,N+1} & 1 \end{pmatrix} \begin{pmatrix} \gamma_{N+1} \\ \xi_{N+1} \end{pmatrix} \tag{3b}$$

$$= \widetilde{M} \begin{pmatrix} \gamma_{N+1} \\ \xi_{N+1} \end{pmatrix}, \tag{3c}$$

$$\widetilde{M} = \frac{1}{t_1 t_2 \ldots t_{N+1}} \begin{pmatrix} a & b \\ c & d \end{pmatrix}; \tag{3d}$$

$$r = \frac{c}{a}, \qquad t = \frac{t_1 t_2 \ldots t_{N+1}}{a}. \tag{3e}$$

For s-polarized and p-polarized incident light, we obtain

$$T_s = \frac{n_{N+1}\cos\theta_{N+1}}{n_0\cos\theta_0}|t_s|^2, \qquad T_p = \frac{n_{N+1}\cos\theta_{N+1}}{n_0\cos\theta_0}|t_p|^2. \tag{4}$$

$$R_s = |r|^2. \tag{5}$$

Here we propose a reconstruction correction technique by retrieving multi-layer wavefront information using the range gated system as shown in Figure 3. After the camera gate width is set to equal to the pulse length, the Shack-Hartmann wavefront sensor samples the incident wavefront from different interfaces at its time-of-flight gating. The wavefront is spatially sampled and focused by lenslet array on the camera. The wavefront from different surfaces can be distinguished based on the range estimation [39]. The front surface is reconstructed. We can estimate the internal coordinate using recursive algorithm to reconstruct the other layer surface. In this case, the wavefront from different layers can be detected and the respective surfaces can be reconstructed.

The multi-layer surface reconstruction algorithms (2 layers case) flowchart is shown in Figure 3. Considering a flat wafer which has a perfect internal structure, we assume that Layer 2 is wafer and the medium in Layer 1 and Layer 3 is air (see Figure 4). The wavefront propagates through the wafer with angle θ_1. Once it hit the interface 1, it will reflect as r_1. Simultaneously, the transmitted wave will continue the propagation. Once it reaches the interface 2, part of the beam will be reflected and travels back to interface 1. Yet again, part of the beam will be transmitted through the interface as t_1. This process will go on till the transmittance $t_N + 1$.

As mentioned by the Snell's law of reflection in Equation (2) with $(i = 1,2,3,4,5)$, $n_5 = n_1, n_4 = n_2$ are considered for 2 layer case. As top surface location x_1, the Snell's law will be considered along the tangent surface taking into consideration the following relations of the roughness angles β_i's on various layers reflection:

$$n_1\sin(\theta_1 - \beta_1) = n_2\sin(\theta_2 - \beta_1), \tag{6}$$

$$n_2\sin(\theta_2 - \beta_2) = n_3\sin(\theta_3 - \beta_2), \tag{7}$$

$$n_2\sin(\theta_4 - \beta_3) = n_1\sin(\theta_5 - \beta_3). \tag{8}$$

The relation between θ_2 and θ_4 is

$$\theta_2 - \beta_2 = \theta_4 + \beta_2 \quad or \quad \theta_4 = \theta_2 - 2\beta_2. \tag{9}$$

From the assumption on smallness of surface roughness, we have the approximation

$$\sin\beta_i \approx \beta_i, \cos\beta_i \approx 1, \qquad i = 1,2,3. \tag{10}$$

As shown in Figure 4, by taking the projection of x_1, x_2, to x_3, the expansion of $(7) - (9)$ with substitution in (10) and (11), we have

$$n_1(\sin\theta_1 - \beta_1\cos\theta_1) = n_2(\sin\theta_2 - \beta_1\cos\theta_2), \tag{11}$$

$$n_2(\sin\theta_2 - \beta_2\cos\theta_2) = n_3(\sin\theta_3 - \beta_2\cos\theta_3), \tag{12}$$

$$n_1(\sin\theta_5 - \beta_5\cos\theta_5) = n_2(\sin\theta_2 - (2\beta_2 + \beta_3)\cos\theta_2). \tag{13}$$

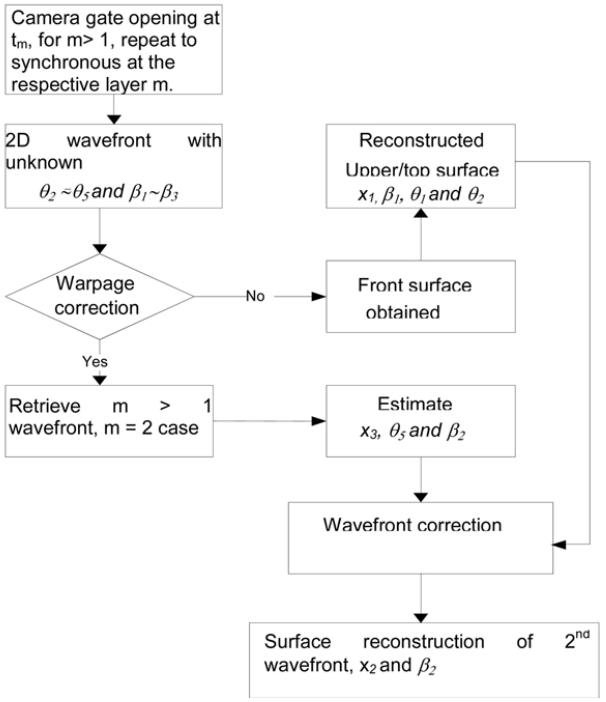

FIG. 3 Multilayer wavefront reconstruction algorithm flowchart (2 layers case) with proposed correction technique.

From $(12)-(14)$, we have that

$$\beta_1 = \frac{n_1 \sin\theta_1 - n_2 \sin\theta_2}{n_1 \cos\theta_1 - n_2 \cos\theta_2}. \tag{14}$$

$$\beta_2 = \frac{n_2 \sin\theta_2 - n_3 \sin\theta_3}{n_2 \cos\theta_2 - n_3 \cos\theta_3}. \tag{15}$$

$$\beta_3 = \frac{n_1 \sin\theta_3 - n_2 \sin\theta_2 + 2n_2\beta_2 \cos\theta_2}{n_1 \cos\theta_5 - n_2 \cos\theta_2}. \tag{16}$$

We shall further make smallness assumption on θ_i's:

$$\sin\theta_i \approx \theta_i, \cos\theta_i \approx 1, \qquad i = 1,2,3,4,5. \tag{17}$$

$(15)(17)$ shall then be further reduced to

$$\beta_1 = \frac{n_1\theta_1 - n_2\theta_2}{n_1 - n_2}, \tag{18}$$

$$\beta_2 = \frac{n_2\theta_2 - n_3\theta_3}{n_2 - n_3}, \tag{19}$$

$$\beta_3 = \frac{n_1\theta_5 - n_2\theta_2 + 2n_2\beta_2}{n_1 - n_2}. \tag{20}$$

For location x_3,the exit wavefront can be derived from (19) and (21), we have that

$$\theta_2 = \frac{1}{n_2}(n_1\theta_1 - (n_1 - n_2)\beta_1), \tag{21}$$

$$\beta_2 = \frac{1}{2n_2}(\beta_3(n_1 - n_2) - (n_1\theta_5 - n_2\theta_2)). \tag{22}$$

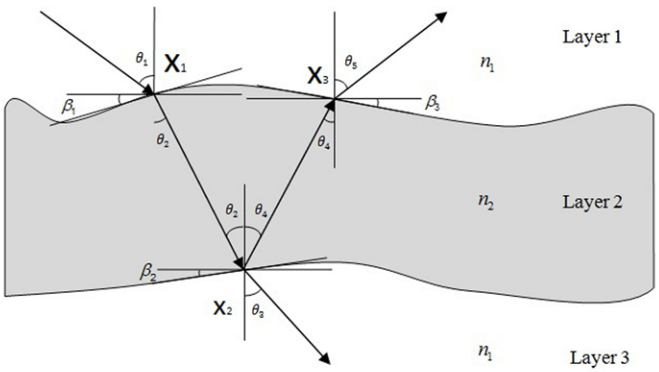

FIG. 4 Multiple reflections in an arbitrary wafer layer (two layers case as an example) of refractive index n_2.

Given the refractive index indicates n_1, n_2; β_1, β_3 can be reconstructed from the first wavefront. Incoming wave is assumed to be non-interferometric and collimated wavefront with incident angle θ_1. θ_2 can be obtained from (13), θ_5 can be reconstructed from the second wavefront, then we are able to estimate the surface waviness of interface 2 which is the slope β_2.

4 SIMULATION RESULTS

From Figure 4, it is clear that the wavefront that passes through upper layer(s) will be distorted (at least twice) due to the discrete surface interfaces. If the wavefront distortion was not corrected, the reconstructed bottom wavefront might carry the upper surface information even in very low surface variation condition. In order to simulate and visualize the condition, the randomly generated wavefront are reconstructed using Xu algorithm [41]. The slope data are extracted to make both top and bottom surface identical. The same surface profile is used to ease the explanation of the simulation result as we should obtain the same surface profile from both corrected and un-corrected case.

For reflected wavefront that has been distorted (top and bottom), the simulation result of two layers discrete medium reconstruction without (blue) / with (red) the proposed correction technique (cross section) is compared with the ideal simulated surface. Figure 5(a) shows the cross section of ideal simulated surface before distortions have happened.

This profile was computed from the wavefront measurement using Southwell [37] approach. It is observed that the lower surface was reconstructed with top surface information as the gated wavefront of the bottom surface has suffered from top surface deviation. Subsequently, the correction using Equation (21) and (22) of the surface wavefront was reconstructed using our proposed compensation technique. From Figure 5(b), we can see that the absolute error is much smaller after using the proposed correction technique. The results show that the correction can achieve 2 order of absolute different from the layer variation in vertical scale. This is because the reconstructed profile has been heavily distorted by the upper layer profile. The corrected surface (bottom layer)

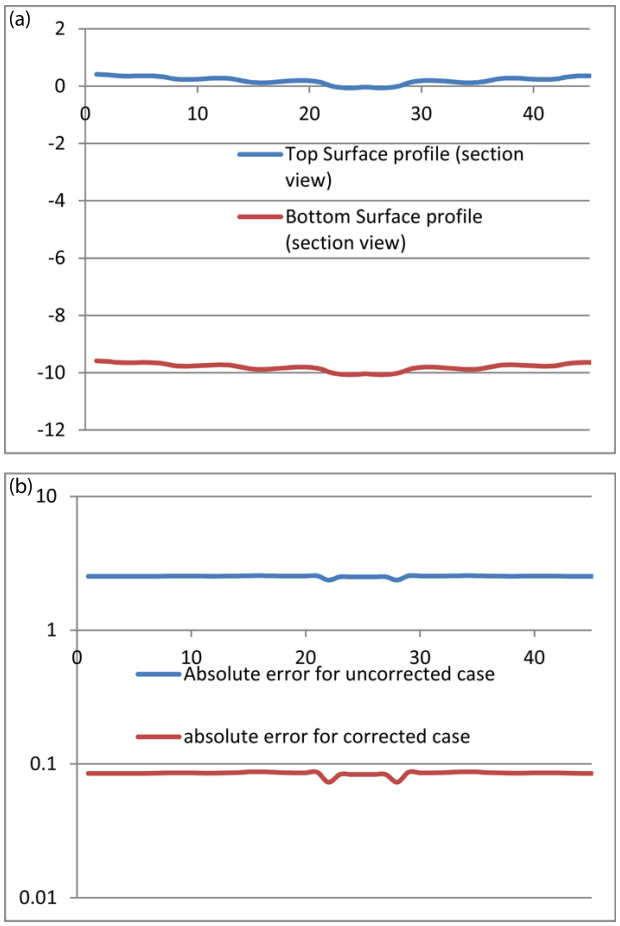

FIG. 5 (a) Cross section of the reconstructed first surface and the actual second surface (both surfaces are duplicated). (b) Comparison between reconstructed second surface (uncorrected) and correct second surface to the actual second surface.

has included the error from the original surface as shown in the simplification of Equation (17).

5 CONCLUSIONS

In this paper, gated wavefront sensing system for multi-layer wave-front sensing is proposed. The method uses a gated camera in a hypothetically pico/femto second shutter that can be synchronized to a pico/femto second laser pulse, up to μm/nm accuracy (not reported in this paper). The correction technique is proven to be needed as the distortion errors (due to upper surface) are up to two logarithmic orders as shown in Figure 5(b), based on simulated profile of Xu algorithm [41]. A numerical model using time-of-flight wavefront sensing is developed to reconstruct the multi-layer surfaces using our proposed gated imaging technique. Further investigation using this numerical model shows that the multi-layer wave-front sensing is possible with time gated wavefront technique.

For future works, various non-ideal conditions should be considered in the multi-layer distortion issues. The multi-layer distortion correction introduced in this paper is for the ideal case of a simulated 2-layer discrete system where the error is converged to less than 0.1 absolute difference of vertical error of surface roughness.

6 ACKNOWLEDGEMENTS

The authors gratefully acknowledge the support and funding from Center for VLSI, University of Tunku Abdul Rahman, Fulbright Foundation, and Ministry of Higher Education Malaysia under Grant No: FRGS/1/2013/SG02/MUSM/02/1.

References

[1] S. Tuohy, and A. Podoleanu, "Depth-resolved wavefront aberrations using a coherence-gated shack-hartmann wavefront sensor," Opt. Express **18**, 3458–3476 (2010).

[2] J. Wang, and A. Podoleanu, "Time-domain coherence-gated Shack-Hartmann wave-front sensor," Proc. SPIE **8091**, 80911L (2011).

[3] N. Goloborodko, V. Grygoruk, V. Kurashov, D. Podanchuk, A. Goloborodko, and M. Kotov, "Determination of surface defects by using the wavefront scanner," Quantum Electronics and Optoelectronics **13**, 65–69 (2010).

[4] N. Bai, L. Zhao, and P. Fang, "Digital shack-hartmann wavefront sensor for toroidalsurface measurement," Proc. SPIE. **6616**, 661644 (2007).

[5] T. Raymond, D. Neal, D. Topa, and T. Schmitz, "High-speed non-interferometric nanotopographic characterization of Si wafer surfaces," Proc. SPIE **4809**, 208–216 (2002).

[6] A. Nutsch, L. Pfitzner, T. Grandin, X. Levecq, and S. Bucourt, "Determination of atness on patterned wafer surfaces using wavefront sensing methods," Proc. SPIE. **7155**, 71550Z (2008).

[7] A. Nutsch, S. Bucourt, T. Grandin, I. Lazareva, and L. Pfitznera, "Wavefront sensor for highly accurate characterization of atness on wafer surfaces," in *Proceedings of the International Conference on Frontiers of Characterization and Metrology for Nanoelectronics*, 188–192 (NIST, New York, 2009).

[8] K. Nemoto, K. Watanabe, T. Hayashi, K. Tsugane, and Y. Tamaki, "Impact of silicon surface roughness on device performance and novel roughness measurement method," in *Proceedings of the Advanced Semiconductor Manufacturing Conference*, 157–160 (IEEE/SEMI, Stresa, 2007).

[9] M. Nagel, A. Michalski, and H. Kurz, "Contact-free fault location and imaging with on-chip terahertz time-domain reectometry," Opt. Express **19**, 12509–12514 (2011).

[10] C. Duran, A. Maznev, G. Merklin, A. Mazurenko, and M. Gostein, "Infrared reectometry for metrology of trenches in power devices," in *Proceedings of the Advanced Semiconductor Manufacturing Conference*, 175–179 (IEEE/SEMI, Stresa, 2007).

[11] C. Chen, D. Lee, T. Pollock, and W. Whitaker, "Pulsed-terahertz reectometry for health monitoring of ceramic thermal barrier coatings," Opt. Express **18**, 3477–3486 (2010).

[12] Y. Ghim, A. Suratkar, and A. Davies, "Reectometry-based wavelength scanning interferometry for thickness measurements of very thin wafers," Opt. Express **18**, 6522–6529 (2010).

[13] J. Fontaine, J. Diels, C. Wang, and H. Sallaba, "Subpicosecond-time-domain reectometry," Opt. Lett. **6**, 405–407 (1981).

[14] A. Liu, P. Wayner, and J. Plawsky, "Image scanning ellipsometry for measuring non-uniformfilm thickness profiles," Appl. Optics **33**, 1223–1229 (1994).

[15] K. Haines, and B. Hilderbrand, "Contour generation by wavefront reconstruction," Phys. Lett. **19**, 10–11 (1965).

[16] H. Fujiwara, *Spectroscopic Ellipsometry Principles and Applications* (Wiley, New Jersey, 2007).

[17] U. Neuschaefer-Rube, W. Holzapfel, and F. Wirth, "Surface measurement applying focusing reection ellipsometry: configurations and error treatment," Measurement **33**, 163–171 (2003).

[18] W. Teh, D. Marx, D. Grant, and R. Dudley, "Backside infrared interferometric patterned wafer thickness sensing for through-silicon-via (TSV) etch metrology," IEEE T. Semiconduct. M. **23**, 419–422 (2010).

[19] M. Tsai, F. Chong, J. Lee, H. Wang, and C. Lee, "Defect detection and property evaluation of indium tin oxide conducting glass using optical coherence tomography," Opt. Express **19**, 7559–7566 (2011).

[20] P. De Groot, and L. Deck, "Three-dimensional imaging by sub-Nyquist sampling of white-light interferograms," Opt. Lett. **18**, 1462–1464 (1993).

[21] N. Tolk, M. Alles, R. Pasternak, X. Lu, R. Schrimpf, D. Fletwood, R. Dolan, and R. Stanley, "Oxide interface studies using second harmonic generation," Microelectron. Eng. **84**, 2089–2092 (2007).

[22] M. Alles, R. Pasternak, X. Lu, N. Tolk, R. Schrimpf, D. Fletwood, R. Dolan, and R. Stanley, "Second harmonic generation for noninvasive metrology of silicon-oninsulator Wafers," IEEE T. Semiconduct. M. **20**, 107–113 (2007).

[23] M. Peterson, P. Hayes, I. Martinez, L. Cass, J. Achtyl, E. Weiss, and F. Geiger, "Second harmonic generation imaging with a kHz amplifier," Opt. Mater. **1**, 57–66 (2011).

[24] X. Li, L. Zhao, Z. Fang, A. Asundi, and X. Yin, "Surface measurement with Shack-Hartmann wavefront sensing technology," Proc. SPIE **7155**, 715515 (2008).

[25] C. Xu, N. Himebaugh, P. Kollbaum, L. Thibos, and A. Bradley, "Validation of a clinical Shack-Hartmann aberrometer," Optometry Vision Sci. **80**, 587–595 (2003).

[26] L. Carvalho, "Accuracy of Zernike polynomials in characterizing optical aberrations and the corneal surface of the eye," Inves. Ophth. Vis. Sci. **46**, 1915–1926 (2005).

[27] S. Furman, and A. Tikhonravov, *Basic of Optics of Multilayer Systems* (Editions Frontieres, Gif-sur-Yvette Cedex, 1992).

[28] O. Heavens, "Computation of periodic multilayers," Opt. Acta **33**, 1463–1465 (1986).

[29] M. Born, and E. Wolf, *Principles of Optics: Electromagnetic Theory of Propagation, Interference and Diffraction of Light* (Cambridge University Press, Cambridge, 1999).

[30] O. Heavens, "The propagation of lateral waves in absorbing media and thin films," J. Mod. Opt. **21**, 1–9 (1974).

[31] B. Sernelius, *Surface Modes in Physics* (Wiley, Berlin, 2001).

[32] L. Jolissain, "Synthetic modeling of astronomical closed loop adaptive optics," J. Europ. Opt. Soc. Public. **5**, 10055 (2010).

[33] V. Paeder, T. Scharf, H. Reffieux, P. Herzig, R. Voelkel, and K. Weible, "Microlenses with annular amplitude and phase masks," J. Europ. Opt. Soc. Public. **2**, 07005 (2007).

[34] H. Hirayama, K. Kaneda, H. Yamashita, Y. Yamaji, and Y. Monden, "Visualization of optical phenomena caused by multilayer films with complex refractive indices," in *Proceedings of the 7th Pacific Conference on Computer Graphics and Applications*, 504–509 (IEEE, Seoul, 2002).

[35] W. Drexler, and J. Fujimoto, *Optical Coherence Tomography: Technology and Applications* (Springer, Heidelberg, 2008).

[36] W. Southwell, "Wave-front estimation from wave-front slope measurements," J. Opt. Soc. Am. **70**, 1917–1983 (1980).

[37] D. Neal, and J. Mansell, "Application of Shack-Hartmann wavefront sensors to optical system calibration and alignment," in *Proceedings of the 2nd International Workshop on Adaptive Optics for Industry and Medicine* 234–243 (World Scientific, Durham, 1999).

[38] J. Busck, and H. Heseiberg, "Gated viewing and high-accuracy three-dimensional laser radar," Appl. Optics **43**, 4705–4710 (2004).

[39] F. Abeles, "Sur la propagation des ondeselectromagnetiquesdans les Milieus Stratifies," Ann. Phys.-Paris **3**, 504–520 (1948).

[40] K. Ohta, and H. Ishida, "Matrix formalism for calculation of electric field intensity of light in stratified multi-layered films," Appl. Optics **29(13)**, 1952–1959 (1990).

[41] P. Su, "Polynomial fitting method for reducing wavefront slope data," Arizona University. (2009).